Micellar Systems as "Supercages" for Reactions of Geminate Radical Pairs. Magnetic Effects

Nicholas J. Turro* and Gregory C. Weed

Contribution from the Chemistry Department, Columbia University, New York, New York 10027. *Received August 2, 1982*

Abstract: The photochemistry of dibenzyl ketone (DBK) and other molecules capable of producing benzyl radicals and substituted benzyl radicals has been investigated in micellar systems. The cage effect (percent of unscavengeable radical pairs produced by photolysis) was measured under a variety of conditions, and the results are compared with those obtained in homogeneous organic solvents. For example, parameters such as mean occupancy of ketone, detergent type and concentration, O_2 concentration, additives, temperature, applied magnetic field, and pressure have been varied and investigated as to their influence on the magnitude of cage effect. In addition to modifying its environment, structural modification of the DBK by incorporation of ^2H and ^{13}C isotopes, hydrophobic groups, and heavy atoms was performed to investigate the impact of these variations on the cage effect in micellar systems. Isotopic substitution of ^2H or ^{13}C leads to results on both the quantum yields for reactions and on the percent cage that were consistent with expectations of magnetic isotope effects. Hydrophobic groups substituted in the 4-position of DBK were found to cause a substantial increase in the cage effect and yet retain the magnetic-field-dependent character found in the parent DBK. Incorporation of Br in the 4-position of DBK was found to enhance the cage effect but at the same time causes the cage effect to become magnetic field independent. Substitution of α-naphthyl for phenyl in DBK also produced magnetic-field-independent behavior, in addition to a dramatic decrease in the efficiency of photolysis.

The Cage Effect

Spin-correlated (singlet or triplet) and composition-correlated (geminate) radical pairs are produced by thermolysis or photolysis of a variety of organic compounds.[1] The "cage effect"[2] may be defined as the fraction of radical pairs produced that undergo reaction within a primary solvent cage. Experimentally, however, the cage effect must be defined in terms of some measurement that monitors the radical pairs that "escape" from the solvent cage, i.e., in terms of the radical pairs that can be scavenged by radical reagents that exist external to the cage in which the radical pairs are born. The experimental cage effect is thus a measure of the competition between escape of the radical pair from its primary solvent cage and reaction in the primary cage.

A "mechanical" picture[3] of the cage effect (Figure 1) provides some insight into the impact of experimental variables on the magnitude of the cage effect. On the basis of the expectation that the cage effect associated with primary singlet radical pairs will be very high ($\sim 100\%$), we shall consider only a model involving primary triplet radical pairs. For example, an increase in viscosity should selectively decrease the rate of escape of the radical pair from the solvent cage, causing more efficient intersystem crossing (ISC) and, therefore, a higher cage effect.[4] Furthermore, if the rate of ISC can be increased (or decreased) relative to the rate of escape in two environments of comparable viscosity, the magnitude of the cage effect will increase (or decrease).

The reactivity of radical pairs toward cage reactions depends critically on the spin state of the caged radical pair. Singlet radical pairs typically undergo efficient cage reactions, whereas triplet radical pairs undergo very inefficient cage reactions.[1] The spin state of a caged radical pair depends on its history and on mechanisms available for preserving, interchanging, or losing spin correlation. In nonviscous ($\eta < 10$ cP) homogeneous solutions at ambient temperature, the lifetimes of solvent cages[2,3] are probably of the order of $\sim 10^{-10}$ s, the time scale for formation of cages by secondary geminate pairs is of the order of $\sim 10^{-8}$ s, and the time scale for formation of caged radical pairs by random radicals is $\gtrsim 10^{-6}$ s. These time scales are important because they determine the temporal framework within which spin correlation is preserved, interchanged, or lost. For example, if a triplet radical pair (^{3}RP in Figure 2) is selectively generated from a triplet (T_1) precursor, a competition is set up between intersystem crossing of the type $^3RP \rightarrow {}^1RP$ within the solvent cage and escape of the radical pair from the cage. Since, typically, triplet–singlet intersystem crossing in a radical pair takes $\sim 10^{-8}$ s, and electronic spin relaxation (by random mechanisms) takes $\sim 10^{-6}$ s, we expect[2,3] that (a) spin correlation is preserved by primary, geminate, radical pairs; (b) spin correlation may be preserved or interchanged, but not lost, by secondary radical pairs; and (c) spin correlation is lost for caged radical pairs formed by random free radicals.

An investigation of the photochemistry of dibenzyl ketone and its derivatives in detergent solutions demonstrated[5c] that triplet benzyl radical pairs produced in micelles behave as if they were located in a special type of solvent cage, i.e., one for which the hydrophobic micelle aggregate served as a restricted space or cage for the radical pair. The measured cage effects were found to be much greater than those found for photolysis in homogeneous solvents whose macroscopic viscosity was comparable to that of the microscopic viscosity of the micelle. This leads to the classification of the hydrophobic micellar aggregate as a "supercage", where the term intends a comparison with the solvent cage provided by a homogeneous solvent of comparable viscosity to that of the micelle.

The goals of this study were to obtain knowledge concerning the variation of the cage effect in micellar systems as a function of the systematic variation of experimental parameters and then to test the validity of the interpretation of the results in terms of the radical-pair theory for homogeneous solution.

Results

Cage effects may be experimentally measured by a number of methods.[6] In our studies, we employed three analyses: (I) a

(1) For a discussion of spin correlation and leading references, see: (a) Fox, J. R.; Hammond, G. S. *J. Am. Chem. Soc.* **1964**, *86*, 4031. (b) Bartlett, P. D.; Porter, N. A. *Ibid.* **1968**, *90*, 5317.

(2) For a discussion and leading references, see: (a) Koenig, T.; Fischer, H. "Free Radicals"; Kochi, J., Ed.; Wiley: New York, 1973; p 157. (b) Noyes, R. M. *J. Am. Chem. Soc.* **1955**, *77*, 2042 **1956**, *78*, 5486. (c) Kaptein, R. *Adv. Free-Radical Chem.* **1975**, *5*, 381.

(3) Frank, J.; Rabinowich, E. *Trans. Faraday Soc.* **1934**, *30*, 120. Rabinowich, E.; Wood, W. *Ibid.* **1936**, *32*, 1381.

(4) Pryor, W. A.; Smith, K. *J. Am. Chem. Soc.* **1970**, *92*, 5403 and references therein.

(5) (a) Photolysis of DBK in homogeneous solution: Engel, P. S. *J. Am. Chem. Soc.* **1970**, *92*, 6074. Robbins, W. K.; Eastman, R. H. *Ibid.* **1970**, *92*, 6076, 6077. (b) Photolysis in micellar systems: Turro, N. J.; Cherry, W. R. *Ibid.* **1978**, *100*, 7431. Turro, N. J.; Kraeutler, B. *Acc. Chem. Res.* **1980**, *13*, 369. (c) Turro, N. J.; Anderson, D. R.; Chow, M.-F.; Chung, C.-J.; Kraeutler, B. *J. Am. Chem. Soc.* **1981**, *103*, 2892.

(6) Sheldon, R.; Kochi, J. *J. Am. Chem. Soc.* **1970**, *92*, 4395. See also the discussions in ref 2a.

0002-7863/83/1505-1861$01.50/0

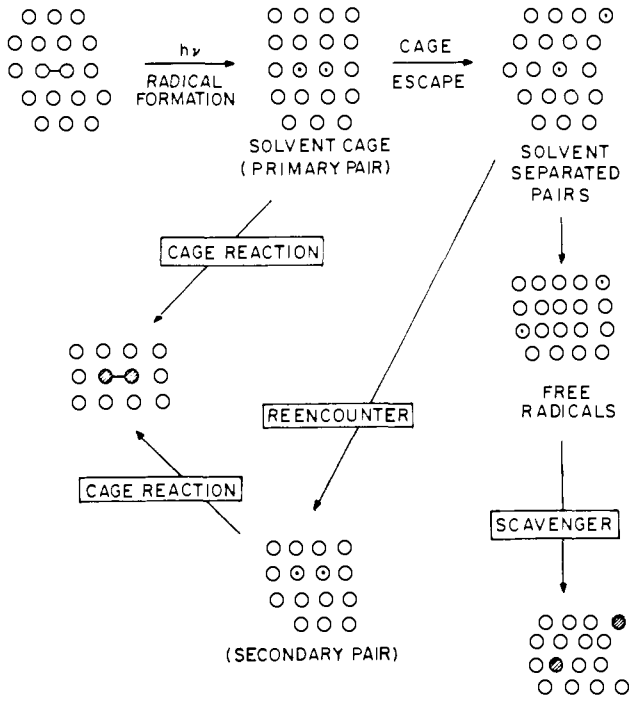

Figure 1. Schematic description of the cage effect in a homogeneous solution. After formation of a solvent-separated radical pair, a competition is set up between formation of free (scavengeable) radicals and return of the pair to a solvent cage. The total cage effect is a measure of primary cage reactions and secondary (and tertiary, etc.) cage reactions.

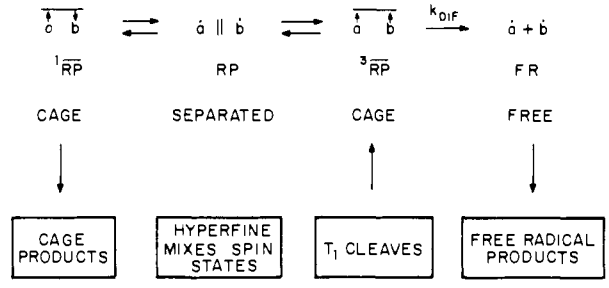

Figure 2. Schematic description of the competition between electron-nuclear hyperfine-induced intersystem crossing (hfi ISC) and diffusion separation of a geminate, triplet radical pair produced by reaction of a molecular triplet (T_1). In the solvent separated form, electron exchange is reduced and hfi ISC can occur.

single-label experiment in which a precursor (ACOB) of the radical pair Ȧ Ḃ is photolyzed to produce a measurable ratio of coupling products AA, AB, and BB; (II) a double-label experiment in which photolysis of a pair of precursors (ACOA and BCOB) initially produces geminate radical pairs ȦA and ḂB, which then proceed to produce a measurable ratio of coupling products AA, AB, and BB; (III) a scavenging experiment in which a selective "out of cage" radical scavenger is employed to determine the fraction of radical pairs that are produced but not scavengeable.

In method I, if an asymmetrical radical pair precursor ACOB is photolyzed to yield coupling products in quantitative yield (eq 1), then the cage effect may be defined in terms of the number of moles of AA, AB, and BB produced according to eq 2.

$$\mathrm{ACOB} \xrightarrow[-\mathrm{CO}]{h\nu} \mathrm{AA} + \mathrm{AB} + \mathrm{BB} \qquad (1)$$

$$\text{cage effect (method I)} \equiv \frac{\mathrm{AB} - (\mathrm{AA} + \mathrm{BB})}{\mathrm{AA} + \mathrm{AB} + \mathrm{BB}} \times 100\% \qquad (2)$$

In method II, for equally absorbing and for equally efficient reactions, if two symmetrical radical-pair precursors ACOA and BCOB are photolyzed to yield coupling products in quantitative yield (eq 3), then the cage effect may be defined in terms of the

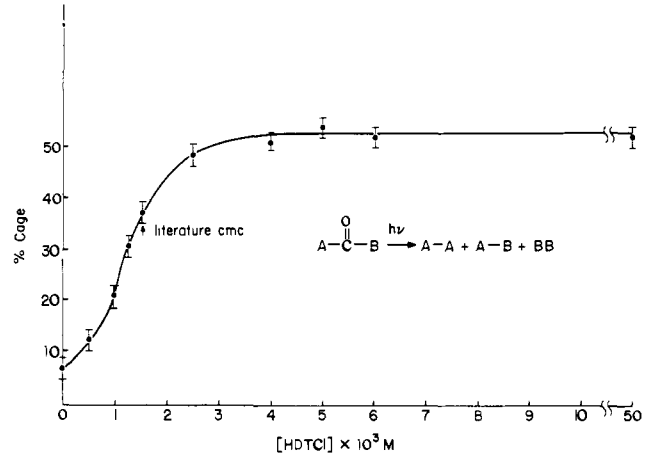

Figure 3. Cage effect for 1.5×10^{-4} M aqueous solution of 4-Me-DBK as a function of [HDTCl] at ambient temperature.

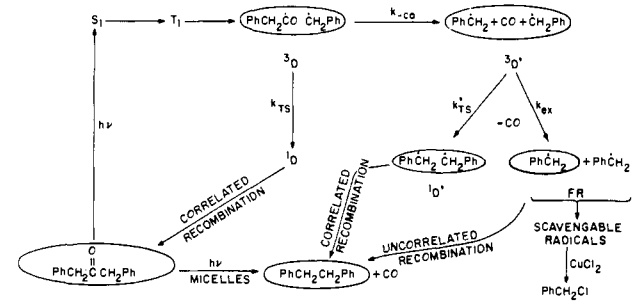

Figure 4. Working mechanism for the photolysis of DBK (and substituted DBK's) in micellar systems. The species enclosed in the ellipses represent micellized reagents, intermediates, or products.

number of moles of AA, AB, and BB produced according to eq 4.

$$\mathrm{ACOA} + \mathrm{BCOB} \xrightarrow[-\mathrm{CO}]{h\nu} \mathrm{AA} + \mathrm{AB} + \mathrm{BB} \qquad (3)$$

$$\text{cage effects (method II)} \equiv \frac{\mathrm{AA} + \mathrm{BB} - \mathrm{AB}}{\mathrm{AA} + \mathrm{AB} + \mathrm{BB}} \times 100\% \qquad (4)$$

In method III, if a radical-pair precursor ACOA is photolyzed to yield the coupling products AA in quantitative yield, then in the presence of a scavenger that selectively and quantitatively reacts with Ȧ radicals that escape the cage, the yield of AA or the yield of the scavenged product may be determined. The cage effect is then conveniently defined as the percent yield of AA where $[\mathrm{ACOA}]_R$ is the yield of reacted ketone according to eq 6.

$$\mathrm{ACOA} + \mathrm{S} \xrightarrow{h\nu} \mathrm{AA} + \mathrm{S\text{–}A} \qquad (5)$$

$$\text{cage effect (method III)} \equiv \frac{\mathrm{AA}}{[\mathrm{ACOA}]_R} \times 100\% \qquad (6)$$

Demonstration of Micellar Effects on the Photolysis of Detergent Solutions of DBK. One of the central demonstrations for the occurrence of micelles in aqueous solution is observation of critical micelle concentration (cmc) behavior.[7] Such behavior is observed (Figure 3) for the photolysis of 1-(4-methylphenyl)-3-phenyl-2-propanone (4-Me-DBK) in aqueous solutions containing the ionic detergents hexadecyltrimethylammonium chloride (HDTCl). Similar behavior is observed for aqueous solutions of sodium dodecyl sulfate ($NaDodSO_4$). The measurements of the cage effect serves as a method for determining the cmc; i.e., the onset of micelles is accompanied by the onset of a significant cage effect. In all of the experiments reported in this paper, the solutions

(7) Fendler, J. H.; Fendler, E. J. "Catalysis in Micellar and Macromolecular Systems"; Academic Press: New York, 1975.

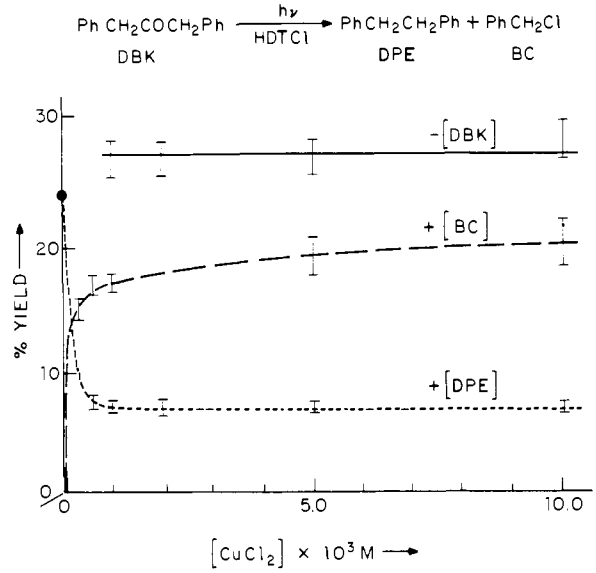

Figure 5. Plots of disappearance of dibenzyl ketone (DBK) and appearance of benzyl chloride (BC) and diphenylethane (DPE) as a function of $CuCl_2$ for the photolysis of aqueous solution of 10^{-3} M DBK and 0.05 M HDTCl. Samples were degassed and photolyzed for equal periods of time on a merry-go-round apparatus.

remained clear and showed no signs of turbidity before or after photolysis. We interpret these results to mean that micelles serve as supercages for the radical pairs produced in the photolysis of 4-Me-DBK.

Cage Effect in the Photolysis of Dibenzyl Ketones and Related Ketones in Micellar Systems. Figure 4 shows the working mechanism for the photolysis of DBK, which will serve as a prototype for all the systems reported here. By the "cage effect" we shall mean the fraction of geminate benzyl radical pairs that combine within a micelle supercage. Typically, the cage effect was measured by the scavenging method (eq 6) for symmetrical ketones and by the product ratio method (eq 2) for unsymmetrical ketones. In all cases reported, the yield of diphenylethanes are >90% of the converted ketone. Figure 4 also shows the idea behind the $CuCl_2$ scavenging experiments for HDTCl solutions. Geminate benzyl radical pairs are produced as a result of an initial homolytic α-cleavage of the triplet ketone, followed by rapid decarbonylation. The scavenger (Cu^{2+} or $CuCl^+$) is active only in the aqueous phase, since the positive charge of the "micelle skin" serves as a Coulombic repulsive barrier to approach of the positively charged scavenger. Radicals that escape into the aqueous phase will either be scavenged or be recaptured by a micelle (which may or may not contain another benzyl radical). At sufficiently high concentration of $CuCl_2$, escape becomes irreversible, i.e., all escaping radicals are scavenged.

Copper(II) chloride proved to be an excellent and practical radical scavenger in HDTCl solution. Photolysis of aqueous HDTCl solutions of DBK in the presence of $CuCl_2$ results in formation of diphenylethane (DPE) and benzyl chloride (BC).[8] Figure 5 shows how the disappearance of DBK, the appearance of DPE, and the appearance of BC depend on $[CuCl_2]$. It is seen that the disappearance of DBK is insensitive to added $CuCl_2$, a result consistent with the inefficient scavenging of geminate $PhCH_2\dot{C}O\ \dot{C}H_2Ph$ radicals that either recombine or decarbonylate but do not escape the micelle "supercage". On the other hand, the yield of DPE appearance decreases and then reaches a limiting value; correspondingly, the yield of BC appearance increases and then reaches a limiting value.

Comparison of Methods Employed To Measure the Cage Effect. It was possible to check the consistency and accuracy of the different methods employed to measure percent cage. It was important to demonstrate that the results obtained with $CuCl_2$ present were not exceptional because of some specific interactions of the scavenger with the micelles. The results were most gratifying and completely consistent with a "passive" role of $CuCl_2$ in all aspects except scavenging radicals that dare to exit into the aqueous phase: For DBK and DBK-2,2′-$^2H_4$ (Scheme I) mixtures, the statistical method (eq 4) yielded a value of 30 ± 2% for the cage reaction, while the $CuCl_2$ scavenging method (eq 6) yielded a value of 31 ± 1%. For 4-Me-DBK, the AA, AB, BB statistical method (eq 1) yielded a value of 52 ± 2%, while the $CuCl_2$ scavenging method for the same ketone (eq 6) yielded a value of 48 ± 4%. For these experiments [HDTCl] = 0.05 M and the [ketone] = 0.001 M. The percent cage was independent of conversion for <30% reaction.

(8) A low yield of benzyl alcohol (about 10% based on DBK consumed) is also formed.

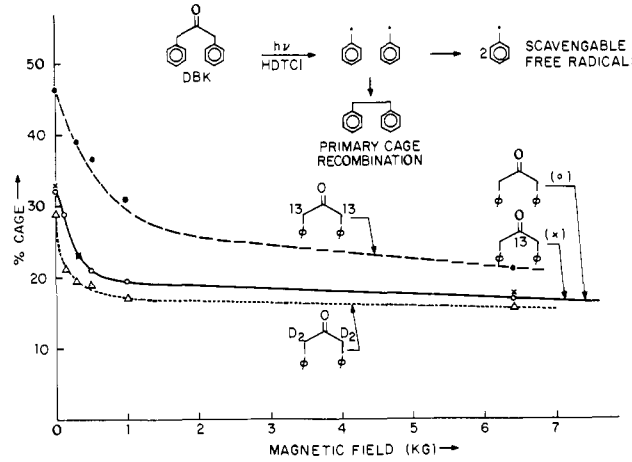

Figure 6. Cage effect ($CuCl_2$ scavenging method) for the formation of DPE as a function of magnetic field for DBK and several isotopically substituted DBK's.

Scheme I

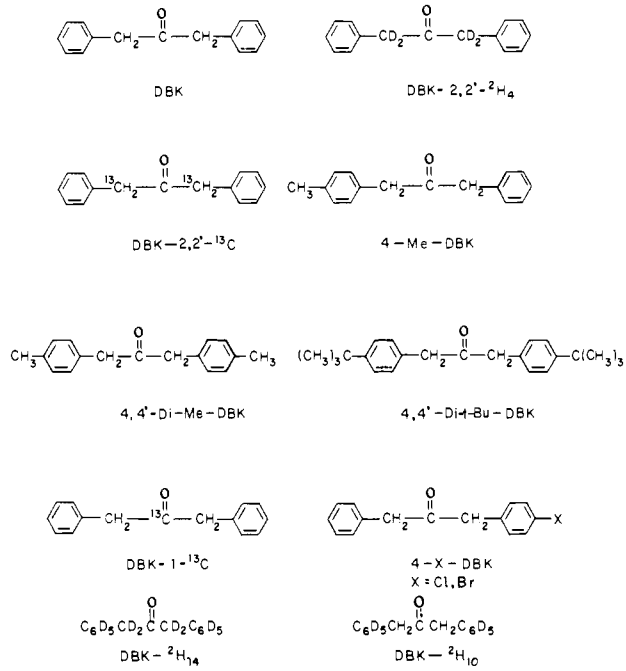

Influence of Magnetic Field on the Cage Effect. The cage effect for DBK in homogeneous organic solutions such as benzene and acetonitrile was found to be equal to zero within experimental error and was not measurably affected by the application of an external laboratory magnetic field. In contrast, the cage effect in micellar solution is exceedingly sensitive to applied laboratory fields (Figure 6). The following qualitative trends are observed for all ketones investigated except 4-Br-DBK (vide infra): the cage effect is maximal in the earth's field (~0.5 G) and then decreases monotonically in the range of ~0–500 G. At about

Table I. Quantum Yields for Photolysis of Dibenzyl Ketones in 0.05 M HDTCl

ketone[a]	Φ_{-K}[b]	cage effect[c] 0 G	cage effect[c] 13 kG
DBK	0.30 ± 0.01	31 ± 1	16 ± 1
DBK-^{13}C	0.22 ± 0.01	31 ± 1	16 ± 1
DBK-2,2′-^{13}C	0.25 ± 0.01	46 ± 3	22 ± 2
DBK-2,2′-$^{2}H_4$	0.32 ± 0.01	29 ± 1	14 ± 1
DBK-$^{2}H_{10}$	0.32 ± 0.01	28 ± 1	
DBK-$^{2}H_{14}$	0.33 ± 0.01	27 ± 1	
4-Me-DBK	0.23 ± 0.01	52 ± 1	31 ± 1
4-Cl-DBK	0.21 ± 0.01	52 ± 1	30 ± 0.6
4-Br-DBK	0.11 ± 0.01	70 ± 4	70 ± 4
4,4′-di-Me-DBK	0.16 ± 0.01	59 ± 3	31 ± 2
4,4′-di-*t*-Bu-DBK	0.13 ± 0.01	95 ± 5	76 ± 5

[a] [Ketone] = 1 mM. [b] Quantum yield for disappearance of ketone in the presence or absence of $CuCl_2$ as scavenger. In the absence of $CuCl_2$, the yield of diphenylethanes is >90% for all ketones listed. [c] Cage effect refers to the efficiency of combination of geminate benzyl radical pairs.

500 G the cage effect approaches a limiting value that is generally reached by 1000 G and that remains constant up to 30 000 G.

These effects are not dependent on micelle structure; i.e., the same qualitative behavior is observed for both HDTCl and NaDodSO$_4$ micelles.

Influence of Isotopic Substitution on Quantum Yields and the Cage Effect. A number of ^{2}H- and ^{13}C-substituted DBK's (Scheme I) were synthesized in order to establish the influence of isotopic substitution of the percent cage, the quantum yield of reaction, and magnetic-field effects. The results for photolysis in HDTCl are summarized in Table I and Figure 6. For DBK as a standard of comparison, Φ_{-K} = 0.30, % cage (0 G) = 31%, and % cage (13 000 G) = 16%. For homogeneous organic solvents,[5] Φ_{-K} is ~0.7 and % cage is ~0. In each case, the yield of DPE was ~90–95% so that the quantum yields for disappearance of ketone and appearance of DPE are nearly identical.

Substitution of ^{13}C at the C-1 position of DBK (DBK-1-^{13}C) causes a substantial decrease in Φ_{-K} but no change in percent cage at 0 G or at 13 000 G. We interpret this result to mean that a ^{13}C magnetic isotope effect occurs in the primary, triplet $PhCH_2\dot{C}O$ $\dot{C}H_2Ph$ radical pair, which causes a *more efficient* recombination than occurs in the natural abundance analogue. The percent cage reflects the behavior of $Ph\dot{C}H_2$ $\dot{C}H_2Ph$ radical pairs only and is not directly related to Φ_{-K}, thus for both DBK and DBK-1-^{13}C the *same* isotopic (natural abundance) radical pair is produced and the percent cage (which measures DPE formation) is independent of isotopic substitution.

Substitution of ^{13}C at both of the C-2 positions of DBK (DBK-2,2-^{13}C) results in a decrease in Φ_{-K} and a dramatic increase in percent cage at both 0 and 13 000 G. We interpret this result to mean that a ^{13}C magnetic isotope effect occurs in *both* the primary $PhCH_2\dot{C}O$ $\dot{C}H_2Ph$ and the secondary $Ph\dot{C}H_2$ $\dot{C}H_2Ph$ radical pairs. The effect of ^{13}C substitution at the 2- (or 2′) position is to cause a *more efficient* recombination than occurs in the natural abundance analogue but a *less efficient* recombination than occurs in the primary radical pair derived from DBK-1-^{13}C. This result is precisely what is expected from inspection of the nuclear–electron hyperfine couplings of the pertinent ^{13}C carbon in the radical pair ($PhCH_2{}^{13}\dot{C}O$, a = 125 G; $Ph{}^{13}CH_2\dot{C}O$, a = 54 G, $Ph{}^{13}\dot{C}H_2$, a = 24 G). The remarkable increase in the percent cage for DPE formation upon ^{13}C substitution at the 2- and 2′-positions is interpreted as a magnetic isotope effect on the recombination of $Ph{}^{13}\dot{C}H_2$ $^{13}\dot{C}H_2Ph$ radical pairs; i.e., ^{13}C enhances the rate of ISC and causes cage recombination to compete more efficiently with escape from the micelle.

The effect of ^{2}H substitution (DBK-$^2H_4$, DBK-$^2H_{10}$, DBK-$^2H_{14}$) on Φ_{-K} and percent cage is small but consistent in the direction of the effects with magnetic isotope effects. Thus, the small *increase* in Φ_{-K} can be explained as resulting from a *less-efficient* intersystem crossing in the primary radical pair due to the *slower intersystem crossing rate* that results from the smaller magnetic moment of ^{2}H relative to ^{1}H. The smaller value of percent cage is also consistent with a less-efficient intersystem crossing of the secondary radical pair. The processes that compete with these ISC's (loss of CO for the primary pair and escape from the micelle for the secondary pair) are not magnetic field dependent and, therefore, become more efficient.

Thus, the effects of ^{13}C and ^{2}H substitution of DBK on Φ_{-K} and percent cage are qualitatively in accord with the occurrence of magnetic isotope effects in the primary and/or secondary radical pairs. In the case of ^{13}C substitution, the effects are much larger than those expected for mass isotope effects. In the case of ^{2}H the effects are small, and the role of ^{2}H mass isotope effects is not known and must await comparison with the predictions of a theoretical model.

Influence of Ring Substitution on Quantum Yields and the Cage Effect. Several ring-substituted DBK's (Scheme I) were synthesized in order to establish the influence of certain groups on the quantum yields, percent cage, and magnetic field effects. In each case, the corresponding diphenylethanes were formed in very good (>90%) yield. The results are summarized in Table I.

Substitution of alkyl groups in the 4-position of DBK causes a reduction in Φ_{-K} and an increase in percent cage. Insufficient information is available to interpret the quantum yield decrease unambiguously; however, the increase in percent cage is nicely correlated with the hydrophobicity of the secondary radical pairs. In the case of 4,4′-di-*tert*-butyl-DBK, *the percent cage is nearly quantitative in the earth's field.* Nonetheless, application of a magnetic field produces a dramatic increase in the percent of escaping radicals. The magnitude of the effect is shown dramatically in terms of the large change in the yield of *p-t*-Bu-$C_6H_4CH_2Cl$ ($CuCl_2$ present) in the presence and absence of a field.

Substitution of chlorine in the 4-position leads to results that are qualitatively similar to those observed with methyl substitution, i.e., a modest reduction in Φ_{-K} and an increase in percent cage. Substitution of bromine in the 4-position, on the other hand, leads to a substantial decrease in Φ_{-K} and a substantial increase in percent cage. Most dramatically, there is no magnetic field dependence on percent cage for the Br-DBK! We interpret these results to mean that chlorine, like methyl, behaves mainly as a modifier of the hydrophobicity of the fragments of the radical pair and has little direct impact on the ISC processes of either radical pair. In contrast, bromine appears to have an exceptional impact on the ISC of *both* the primary and the secondary pairs. From data in the literature, it is natural to ascribe this special feature of bromine substitution to a "heavy atom" effect on ISC.[9] We propose that it is spin–orbit coupling that causes the unusually rapid ISC of T_1 to be induced by bromine substitution. This more rapid ISC in the primary radical pair causes a more efficient recombination and, therefore, a lower Φ_{-K}. Other possibilities such as the introduction of a new radiationless decay from S_1 or T_1 to S_0 (without the formation of radical pairs) are not rigorously ruled out by our data but are rendered unlikely by their absence in precedence.

Similarly, in the secondary pairs, the faster ISC causes a more efficient cage. Furthermore, since in this case the mechanism of ISC is not hyperfine induced, there is no magnetic field dependence on the percent cage. Recent results[10] have shown that the percent cage for 4-Br remains constant from 0 to 145 000 G!

Influence of Detergent Structures on the Cage Effect. The influence of detergent chain length and charge on the cage effect was investigated with 4-Me-DBK as a probe, by employing the statistical method (eq 2). Figure 7 shows that for a series of straight chain sulfate detergents containing from 6 to 14 carbons, the cage effect increases monotonically. These results are consistent with the postulate that the rate of radical escape from a micelle is inversely proportional to the "hydrophobic size" of the micelle, i.e., the hydrocarbon chain length. From literature data,[11]

(9) Closs, G. L.; Doubleday, C. E.; Paulson, D. R. *J. Am. Chem. Soc.* **1970**, *92*, 2185.
(10) Turro, N. J.; Chung, C.-J.; Jones, G.; Becker, W. G. *J. Phys. Chem.* **1982**, *86*, 3677.
(11) Mysels, K. J. *J. Colloid Sci.* **1955**, *10*, 507.

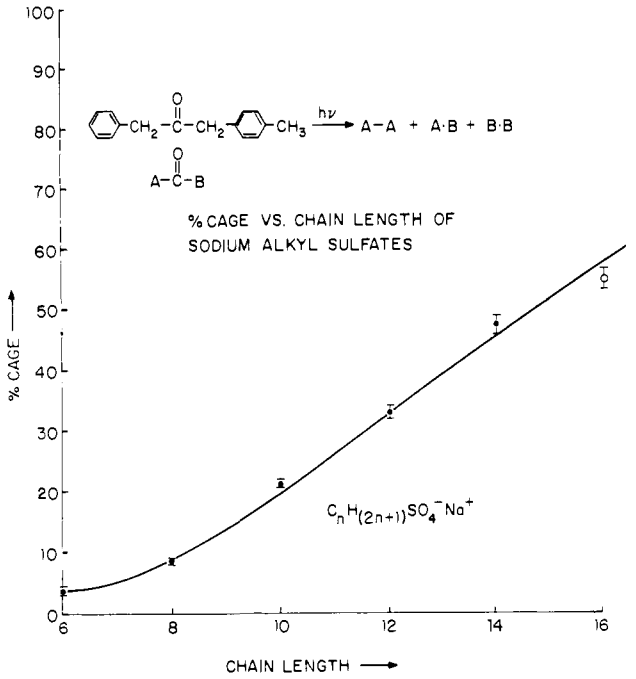

Figure 7. The cage effect for 4-Me-DBK as a function of detergent chain length. For all samples, [DBK] = 10^{-3} M. The detergent concentrations were adjusted so that [micelles] $\simeq 5 \times 10^{-4}$ M. The open circle is the cage effect for HCTCl, a 16-carbon cationic detergent. The 16-carbon sulfate proved to be too insoluble to be included in the group studied.

the micelles formed from each of the detergents investigated have aggregation numbers of the order of 50–100 under the conditions employed.

The cage effect is relatively insensitive to the micelle charge, since values of 30% and 25% were determined for $NaDodSO_4$ and for dodecyltrimethylammonium chloride under comparable conditions. In all cases, the precent cage was decreased to a limiting value by application of a magnetic field in a manner that was qualitatively similar to that found for HDTCl.

Influence of Temperature, Applied Pressure, and Additives. The size, shape, cmc, and other physical properties of micelles are changed by variation of temperature and pressure and additives such as salts or alcohols.[12] For example, for $NaDodSO_4$ micelles, the micellar size and cmc increase with increasing temperature,[13] whereas the application of pressure causes a significant change in micellar "microviscosity".[14] The addition of NaCl causes a reduction of the cmc of $NaDodSO_4$ and also causes an increase in aggregation number and shape of $NaDodSO_4$ micelles.[15] On the other hand, addition of hydrophobic alcohols generally decreases the aggregation number of $NaDodSO_4$ micelles.

Both temperature and pressure exert only a modest influence ($\sim$10% changes) on the cage effect of 4-Me-DBK in $NaDodSO_4$ micelles for temperature changes from 25 to 69 °C and pressure changes from 1 to 2000 bar. The addition of strong electrolytes (NaCl or Na_2SO_4) up to $\sim$0.5 M also causes a modest increase ($\sim$25%) in the cage effect. On the other hand, addition of $PhCH_2OH$ (0.2 M) decreases the cage effect slightly ($\sim$10%). We view these variations to be too small to justify any detailed interpretation.

Influence of Substitution of Naphthyl for Phenyl in DBK. Replacement of one or both of the phenyl groups of DBK resulted in a dramatic decrease in quantum efficiency of photolysis in homogeneous solution. For example,[16] the quantum yield for disappearance of 1,3-di-α-naphthylpropan-2-one (DNP) in

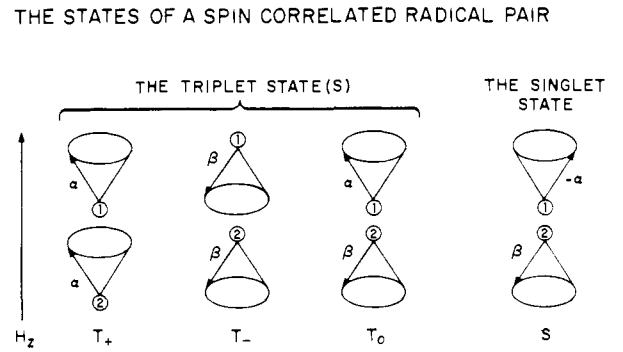

Figure 8. Vector representation of the three magnetic sublevels of a triplet radical pair and the singlet level of a radical pair. α denotes an "up" spin, and β denotes a "down" spin. The $-\alpha$ in the singlet state refers to the completely out of phase precession of the "up" spin relative to the associated "down" (β) spin.

CH_3CN has been reported to be only $\sim$0.001, compared to a value of $\sim$1.0 for DBK. A comparably low quantum yield ($\Phi \sim 0.005$) for DNP is found for photolysis in HDTCl solutions. The cage effect for 1-α-naphthyl-3-phenylpropan-2-one in both CH_3CN and in HDTCl micelles is $\sim$100%, in the earth's field or in a field of 14 000 G. The high value of the cage in CH_3CN and the lack of a magnetic field effect on the cage for phenyl naphthyl ketone in micelles is consistent with *singlet* cleavage. These results may also be explained in terms of conversion to an unreactive π,π^* triplet upon naphthyl substitution but require further quantitative study before a firm conclusion can be made.

Discussion

The "supercage" environment provided by a micellar environment for a triplet geminate radical pair results in a much higher cage effect than that observed in homogeneous solution.[5] In addition, the special restricted space of a micellar aggregate allows the manifestation of magnetic field and magnetic isotope effects on cage reactions.

Investigations of the effect of applied laboratory magnetic fields on organic reactions in solutions has quite generally yielded negative results.[17] The lack of positive results can be readily understood from the fact that the strongest available laboratory fields ($\sim$100 000 G) correspond, at best, to energy differences of the order of $\sim 10^{-2}$ kcal/mol for organic systems,[17] so that neither equilibrium distributions nor rates of passage over energy barriers are expected to be significantly modified by the application of even the strongest laboratory fields. This simple energetic fact of life has served as the underpinning of a healthy pessimism concerning the observation of substantial magnetic field effects on organic chemical reactions. Furthermore, numerous reports of magnetic field effects on reactions have been later retracted or have been found to be irreproducible or very small in magnitude.[18] Finally, convincing physical mechanisms that could lead to substantial magnetic effects on reactions were not apparent. However, the radical-pair theory of CIDNP[19,20] produced a well-defined physical model for understanding circumstances under which significant magnetic field effects on chemical reactions could be sought and even expected.

Mechanistic Origin of Magnetic Effects on Chemical Reactions. It is anticipated that magnetic effects will be significant for reactions involving homolytic cleavage to produce radical pairs because such reactions generate electronic magnetic moments that interact strongly (1) between themselves, (2) with magnetic

(12) Gratzel, M.; Thomas, J. K. *J. Am. Chem. Soc.* **1973**, *95*, 6885.
(13) Murray, R. C.; Hartley, G. S. *Trans. Farad. Soc.* **1935**, *31*, 183.
(14) Turro, N. J.; Okubo, T. *J. Am. Chem. Soc.* **1981**, *103*, 7224.
(15) Lianos, P.; Zana, P. *J. Phys. Chem.* **1980**, *84*, 3339.
(16) Roof, A. A. M.; vanWoerden, H. I.; Cerfontain, H. *J. Chem. Soc., Perkin Trans. 2* **1979**, 1545.

(17) For leading references, see: (a) Atkins, A. W.; Lambert, T. P. *Annu. Rep. Prog. Chem., Sect. A: Phys. Inorg. Chem.* **1975**, 67. (b) Buchachenko, A. L.; *Russ. Chem. Rev. (Engl. Transl.)* **1976**, *45*, 375.
(18) Atkins, P. *Chem. Br.* **1976**, *12*, 214. Figueras Roca, F. *Ann. Chim. (Paris)* **1967**, *2*, 255.
(19) Closs, G. L. *J. Am. Chem. Soc.* **1969**, *91*, 4552. Closs, G. L.; Trifunic, A. D. *Ibid.* **1969**, *91*, 4552. Kaptein, R.; Oosterhoff, L. J. *Chem. Phys. Lett.* **1969**, *4*, 195, 214.
(20) Lawler, R. G. *Acc. Chem. Res.* **1972**, *5*, 25.

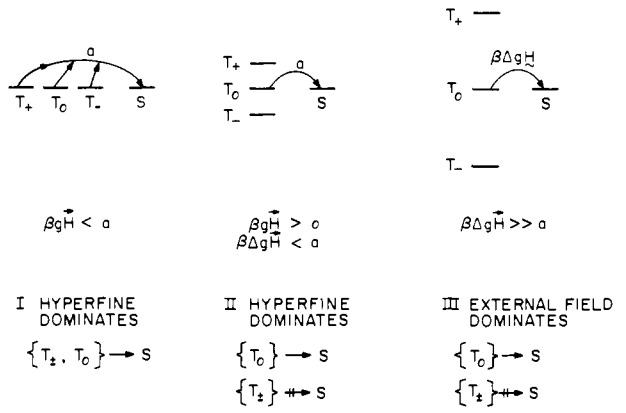

Figure 9. Diagram of the influence of the Zeeman interaction of T ⇄ S intersystem crossing. At zero magnetic field ($\vec{H} < a$), all three triplet levels are energetically degenerate with the singlet state and may undergo electron–nuclear hyperfine-induced intersystem crossing. When $\beta\Delta g\vec{H}$ is large relative to the hyperfine splitting constant a, only $T_0 \rightleftarrows S$ ISC is possible, since the $T_\pm$ levels are split from S. ISC is then determined by the external magnetic field strength when $\beta\Delta g\vec{H} \gg a$.

moments of nuclei, and (3) with laboratory magnetic fields. The mechanistic origin of magnetic field effects on radical reactions is illustrated qualitatively by considering a simple model such as the radical pair RĊO Ṙ produced by α-homolytic cleavage of a ketone.

The radical pair RĊO Ṙ, immediately after its generation, may be classified as a singlet or as a triplet radical pair. The singlet and the three triplet levels of the radical pair may be classified according to a vector model as shown in Figure 8. Triplet-singlet (T–S) intersystem crossing involves conversion of T_+, T_-, or T_0 to S. The vector model suggests that two distinct mechanisms should exist for T–S interconversions: (1) a spin-vector rephasing in which T_0 is converted to S as a result of different precessional rates of the spin vectors and (2) a spin-vector flip by which T_+ and/or T_- is converted to S.

The *rate* of intersystem crossing (k_{TS}) will be a function of magnetic interactions that cause $T_0 \rightarrow S$ to occur.[17] It follows from the radical-pair theory of CIDNP[19,20] that $T \rightarrow S$ intersystem crossing in radical pairs should exhibit the following behavior: (1) the rate of intersystem crossing (k_{TS}) will depend on the magnitude of the external field strength H_0, the Δg value, and the magnitude of the dominant hyperfine-coupling constant a; (2) at "low magnetic fields", $a \gg \Delta g\beta H_0$, only the hyperfine coupling induces intersystem crossing; (3) at "high magnetic fields", $\Delta g\beta H_0 \gg a$ and the rate of $T_0 \rightarrow S$ becomes dependent of a and depends on $\Delta g\beta H_0$ only. It turns out that the rate of $T_\pm \rightarrow S$ intersystem crossing depends on, in an *indirect* fashion, the magnetic field strength, since an external field causes T_+ and T_- to split in energy from S. As a result, $T_\pm \rightarrow S$ interconversions are slowed down at "high fields" (Figure 9).

Figure 10 summarizes two limiting cases for cage effects of geminate triplet radical pairs at "low fields" and at "high fields". In the former case, some fraction, α, of the triplet radical pairs undergoes ISC and undergoes cage reactions (e.g., combination). In the latter case, two-thirds of the radical pairs (T_+ and T_-) are "quenched" from undergoing ISC and one-third of the radical pairs (T_0) maintain their ability to undergo ISC and cage reaction; i.e., if at "low field" the cage effect = α, then at "high field" the cage effect = 0.33α. This latter expectation has been confirmed experimentally.[10]

There is no reason to believe that the supercage provided by a micelle is unique with respect to its ability to promote magnetic effects on the reactions of triplet radical pairs. This expectation has been corroborated in the finding of both magnetic field and magnetic isotope effects in the photolysis of DBK in environments such as porous glass, polymer films, lipid bilayers, and porous silica.[21]

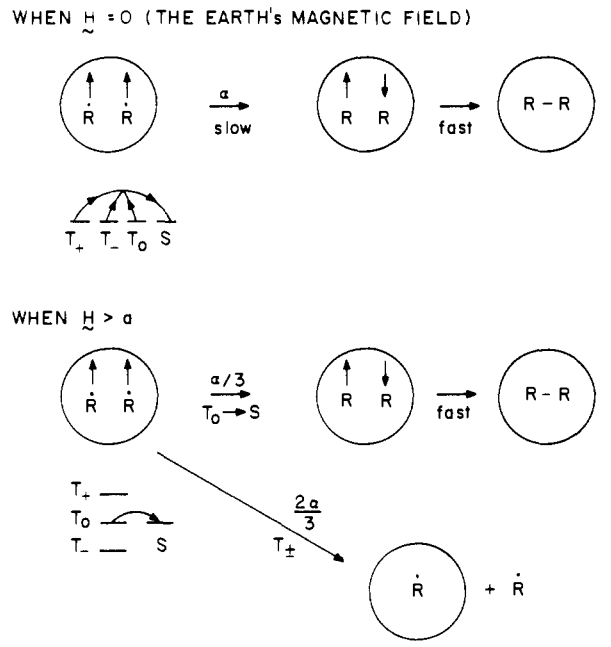

Figure 10. Schematic description of the influence of an applied external magnetic field on the cage effect on a geminate triplet radical pair in a supercage. Extreme situations are represented. At low field, hyperfine-induced ISC can lead to a cage effect of unity, and at high field the "quenching" of ISC for two-thirds of the triplet sublevels could reduce the cage effect to one-third of its initial value.

Experimental Section

Spectroscopy. Proton NMR spectra were taken on Varian T-60 (60 MHz) and Perkin-Elmer R-32 (90 MHz) spectrometers. Chemical shifts are reported in parts per million downfield from tetramethylsilane. UV absorption spectra were recorded on a Cary spectrometer, Model 17.

Solvents and Detergents. Water was doubly distilled (first distillation from $KMnO_4$); benzene (Fisher, "Spectroanalyzed"), isooctane (Aldrich, "Gold Label"), and acetonitrile (MCB Reagents, "Omnisolve") were used without further purification. The detergents hexadecyltrimethylammonium chloride (HDTCl), dodecyltrimethylammonium chloride (DDTCl), sodium tetradecylsulfate (STS), sodium decyl sulfate (SDS), sodium octylsulfate (SOS), and sodium hexylsulfate (SHS) were obtained from Eastman Co., and sodium dodecyl sulfate ($NaDodSO_4$) was procured from Biolab. The detergents were recrystallized from ethanol and dried subsequently under 10^{-2}-torr pressure at room temperature. $CuCl_2$ was obtained from Fisher.

Preparation and Purification of Ketones. 1. Dibenzyl ketone (DBK = natural abundance isotopic composition; Aldrich Chemical Co.) was commercially available material that was sublimed (at a bath temperature of ca. 40 °C and pressure of $\sim 10^{-1}$ torr) to give colorless crystals. The compound was stored as all other ketones in the dark at ~0 °C.

2. 1,3-Diphenylpropan-d_4-2-one (DBK-2,2′-$^2H_4$) was prepared in 75% overall yield (0.96 g) from 1.25 g of dibenzyl ketone (DBK). The 1.25 g of DBK was stirred at reflux temperature for 15 h in a mixture of 5 mL of benzene and 1 mL of 1 M NaOD in D_2O (Aldrich "Gold Label" 99.8 atom % D). Afterwards, 15 mL of ether was added to the reaction mixture and the aqueous portion removed. The organic layer was washed twice with dilute aqueous HCl and then twice with distilled water, followed by drying over magnesium sulfate and evaporation of ether and benzene. The resulting oil was sublimed at 40 °C to yield the product as colorless crystals. The extent of deuteration at the benzylic position was >95% as determined by ^1H NMR (ratio of integrated aromatic and benzylic protons was >50) and mass spectral analysis: MS, m/e (%) 215 (18), 214 (100), 213 (6), 212 (0), 211 (0), 210 (0).

3. 1,3-Di(phenyl-d_5)-2-propan-d_4-one (DBK-$^2H_{14}$) was prepared from phenylacetic-d_7 acid (Merck, Sharpe & Dohme), 98 atom % D.[22] A mixture of 2 g (0.014 mol) of $C_6D_5CD_2CO_2H$ and 0.45 g (0.008 mol) of reduced iron powder (Fisher) was heated in a round-bottom flask at 140 °C for 2 h (under nitrogen). After reaction, the system's pressure was reduced to 0.06 torr and the temperature was raised until distillation of the organic fraction was complete. The distillate was dissolved in ether, washed three times with a saturated aqueous sodium bicarbonate

(21) Turro, N. J.; Baretz, B. H. *J. Am. Chem. Soc.*, in press.

(22) Davis, R.; Schultz, H. P. *J. Org. Chem.* **1962**, *27*, 854.

solution, and then washed two times with distilled water. A white solid residue was recovered after drying with magnesium sulfate and removal of solvent. Product verification was made by gas chromatography (identical retention time as that of the parent ketone), UV absorption (no major changes from the parent), and NMR (extent of deuteration as compared with Cl_3CCH_2OH standard in CCl_4 solvent was 90%). Yield of product was 1.0 g (64%). The product was sublimed in the usual manner for use in experiments: MS, *m/e* (%) 225 (13), 224 (100), 223 (40), 222–210 (0).

4. 1,3-Di(phenyl-d_5)-2-propanone (DBK-$^2H_{10}$) was prepared from 0.1 g (0.4 mmol) of 1,3-di(phenyl-d_5)-2-propan-d_4-one. The 0.1 g of DBK-$^2H_{14}$ was added to 0.5 mL of benzene and 1 mL of 1 M NaOH in H_2O and refluxed for 14 h. Ketone (94 mg) was recovered (as in the procedure of the DBK-$^2H_4$ synthesis), and the extent of benzylic protonation was determined as >99% by ^1H NMR spectroscopy using Cl_3CCH_2OH as standard in CCl_4 solvent. No detectable signal was found in the aromatic region at the sensitivity employed: MS, *m/e* (%) 225 (0), 224 (0), 223 (4), 221 (25), 220 (100), 219 (11), 218–210 (0).

5. 1,3-Bis(4-methylphenyl)-2-propanone (4,4′-di-Me-DBK) was prepared from (4-methylphenyl)acetic acid (Aldrich). The acid (7.0 g, 47 mmol) and 1.4 g (25 mmol) of reduced iron (Fisher) were mixed together and heated at 140 °C under a N_2 atmosphere for 1 h. The vacuum distillate that resulted was treated as in the DBK-$^2H_{14}$ synthesis to isolate the ketone. Yield of sublimed product was 23% (2.55 g): ^1H NMR (90 MHz, $CDCl_3$) δ 7.0–7.4 (m, 8 H), 3.66 (s, 4 H), 2.33 (s, 6 H).

6. 1-(4-Methylphenyl)-3-phenyl-2-propanone (4-Me-DBK). A 12.0-g (0.080 mol) sample of 4-(methylphenyl)acetic acid (Aldrich) was placed in a round-bottom flask, and 12 mL (0.016 mol) of $SOCl_2$ (Fisher) was added dropwise at room temperature. The mixture was refluxed for 1 h, and excess $SOCl_2$ was distilled off. The resulting 4-methylphenylacetyl chloride was vacuum distilled to yield 95% (13 g) of pure reagent: ^1H NMR (60 MHz, $CDCl_3$) δ 7.15 (s, 4 H), 4.07 (s, 2 H), 2.35 (s, 3 H). A 21-mL (0.182 mol) sample of benzyl chloride (Fisher) in 90 mL of ether (anhydrous) was added to a three-necked round-bottom flask (equipped with condenser, overhead stirrer, and dropping funnel) that contained 4.5 g (0.185 mol) of magnesium turnings, 20 mL of ether, and a few iodine crystals. Addition was complete over a 30-min period with continuous stirring. Cadmium chloride (34.5 g, 0.188 mol) (Fisher) was added over a 15-min period as the reaction mixture was stirred and ice cooled. Stirring was continued at temperatures less than 10 °C for 2 h. Then, 13 g (0.076 mol) of (4-methylphenyl)acetyl chloride in 35 mL of ether was added over a period of 10 min. The reaction mixture was flushed with N_2 and stirred below 10 °C over a period of 6 h. Next, 105 mL of 10% H_2SO_4 was added and the ether layer separated while the aqueous layer was washed (3 × 20 mL) with ether. The ether extracts were washed with 5% aqueous sodium bicarbonate, water, and then saturated NaCl in H_2O. The solvent was removed and the resiidual yellow oil was distilled in vacuo. Impurities were separated from the distillate on a silica gel column using 5% (v:v) ether in hexanes. A 67% (11.4 g) overall yield of the ketone was obtained: ^1H NMR (60 MHz, $CDCl_3$) δ 7.0–7.4 (m, 9 H), 3.64 (s, 2 H), 3.61 (s, 2 H), 2.30 (s, 3 H).

7. 1-(4-Chlorophenyl)-3-phenyl-2-propanone (4-Cl-DBK) was synthesized in the same manner as 4-Me-DBK.[23] (4-Chlorophenyl)acetyl chloride (15.6 g, 0.082 mol) prepared quantitatively from (4-chlorophenyl)acetic acid (Aldrich) was reated with 0.200 mol of the benzylcadmium reagent [$(PhCH_2)_2Cd$], yielding after workup 26% ketone (5.9 g) as colorless crystals: ^1H NMR (MHz, $CDCl_3$) δ 7.0–7.4 (m, 9 H), 3.67 (s, 2 H), 3.62 (s, 2 H).

8. 1-(4-Bromophenyl)-3-phenyl-2-propanone (4-Br-DBK) was synthesized in the same manner as 4-Me-DBK. (4-Bromophenyl)acetyl chloride (6.4 g, 0.027 mol) prepared quantitatively from (4-bromophenyl)acetic acid (Aldrich) was reacted with 0.067 mol of benzylcadmium to yield after workup ~30% ketone (2.2 g) as colorless crystals: ^1H NMR (90 MHz, $CDCl_3$) δ 6.9–7.5 (m, 9 H), 3.64 (s, 2 H), 3.58 (s, 2 H).

9. 1,3-Bis(4-*tert*-butylphenyl)-2-propanone (4,4′-di-*t*-Bu-DBK) was prepared in the following sequence:

A. Preparation of 4-*tert*-Butylbenzyl Cyanide. Thirty grams (0.132 mol) of 4-*tert*-butylbenzyl bromide (Fluka) and 28 mL of ethanol were added to 9.8 g (0.131 mol) of potassium cyanide (J. T. Baker) in 10 mL of distilled water. After a 3-h reflux, the mixture was cooled and separated from KBr by filtration. The solvent was removed from the filtrate, and an NMR spectrum was taken of the residue: ^1H NMR (60 MHz, $CDCl_3$) δ 7.25 (s, 4 H), 3.62 (2, 2 H), 1.33 (s, 9 H).

B. Preparation of (4-*tert*-Butylphenyl)acetic Acid. Acid. Twenty-three grams (0.132 mol) of 4-*tert*-butylbenzyl cyanide was heated with 80 mL of a 2:3 (v:v) mixture of water and concentrated sulfuric acid at reflux temperature for 15 min. The mixture was cooled, diluted with water, and then extracted with ether. The ether layer was washed with water and dried over magnesium sulfate, and the ether was removed. The acid was obtained in quantitative yield (25 g): ^1H NMR (60 MHz, $CDCl_3$) δ 7.90 (s, 1 H), 7.25 (m, 4 H), 3.60 (s, 2 H), 1.33 (s, 9 H).

C. Preparation of (4-*tert*-Butylphenyl)acetyl Chloride. A 22.5-g (0.012 mol) sample of (4-*tert*-butylphenyl)acetic acid was refluxed for 1 h with 17 mL (0.023 mol) of thionyl chloride. Unreacted thionyl chloride was removed, followed by distillation, in vacuo, of the acetyl chloride in near-quantitative yield (24 g): ^1H NMR (60 MHz, $CDCl_3$) δ 7.0–7.4 (m, 4 H), 4.07 (s, 2 H), 1.32 (s, 9 H).

D. Preparation of 1,3-Bis(4-*tert*-butylphenyl)-2-propanone (4,4′-di-*t*-Bu-DBK). The 4-*tert*-butylbenzylcadmium reagent was prepared from 35.5 g (0.156 mol) of 4-*tert*-butylbenzyl bromide and was reacted with 13.7 g (0.065 mol) of (4-*tert*-butylphenyl)acetyl chloride in a procedure analogous to that described for the synthesis of 4-Me-DBK. The residue obtained was a mixture of 4-*tert*-butyltoluene, 1,2-bis(4-*tert*-butylphenyl)ethane, and the desired ketone. The toluene was removed by vacuum distillation, and the remaining residue was crystallized from hexanes. The ketone was separated on a silica gel column with 5% (v:v) ether–hexanes. The reaction yielded ~60% (12.6 g) of ketone: ^1H NMR (90 MHz, $CDCl_3$) δ 7.0–7.4 (m, 8 H), 3.67 (s, 4 H), 1.32 (s, 18 H).

10. 1-Phenyl-3-(1-naphthyl)-2-propanone (PNK) was prepared essentially in the same manner as 4-Me-DBK—7.9 g (0.038 mol) of 1-naphthylacetyl chloride, prepared quantitatively from 1-naphthylacetic acid, was reacted with 0.093 mol of benzylcadmium to yield after workup ~20% ketone (1.0 g) as a crystalline residue. Before use in experiments, the crystalline product was sublimed: ^1H NMR (90 MHz, $CDCl_3$) δ 7.0–7.8 (m, 12 H), 4.12 (s, 2 H), 3.65 (s, 2 H).

11. 1,3-Di-(1-naphthyl)-2-propanone (DNK) was prepared in a two step synthesis as follows:

A. 1-Naphthylacetic anhydride was prepared from the parent carboxylic acid (Aldrich) by refluxing in acetic anhydride and removing by way of distillation the resulting acetic acid:[24] ^1H NMR (90 MHz, $CDCl_3$) δ 7.2–8.2 (m, 14 H), 3.68 (s, 4 H).

B. 1,3-Di-(1-naphthyl)-2-propanone (DNK) was prepared in 27% yield (lit. 32%)[25] by photolysis of argon-purged 0.03 M (1.1 g anhydride (3 mmol) in 100 mL of solvent) 1-naphthylacetic anhydride in acetonitrile (MCG Reagents "Omnisolve") in a quartz vessel for 11.5 h. The light source was a 450-W medium-pressure mercury vapor lamp set in a quartz cooling jacket. The photolysis was monitored by ^1H NMR. After photolysis, the acetonitrile was removed, and the resultant residue was purified on a silica gel column with 59% (v:v) CH_2Cl_2 in hexanes. A total of 238 mg (0.8 mmol) of the ketone was separated from other photoproducts (ester and dinaphthylethane): ^1H NMR (90 MHz, $CDCl_3$) δ 7.2–8.2 (m, 14 H) and 4.14 (s, 4 H).

Standard Photolysis Experiments. 1. "Merry-Go-Round" Experiments (Earth's Magnetic Field = 0.5 G). Ketones. Quantum yield determinations and scavenging studies were carried out by using a "merry-go-round" apparatus ("Turntable Photochemical Reactor", Ace Glass Co., Inc. Vineland, NJ) immersed into an ambient-temperature (25 °C) water bath. A 450-W medium-pressure Hanovia Hg lamp was employed as the light source from which 313-nm light was selected by means of an aqueous chromate filter (0.27 g/L potassium chromate–1 g/L sodium carbonate)[26] and Corning 7-54 filters. All quantum yields reported in the text were determined on the basis of relative quantum yields by using DBK as the actinometer possesssing literature quantum yields of 0.070 and 0.30 in benzene (or dioxane) and 0.05 M HDTCl, respectively. Generally, 2 mL of N_2-purged sample solutions, micellar (usually 0.05 M HDTCl) or homogeneous, containing 0.001 M ketone (2.0×10^{-4} M for 4,4′-di-*t*-Bu-DBK) were photolyzed to 15–30% conversion in rubber-stoppered 100 mm × 13 mm Pyrex test tubes. When micellar $CuCl_2$ scavenging experiments were performed, samples with and samples without scavenger were photolyzed simultaneously.

2. Experiments at Applied Magnetic Field. Magnetic field experiments were performed with an Alpha Scientific, Inc., Model 4500 4-in., adjustable-gap electromagnet. Calibrations were made with a Bell Model 640 gaussmeter. Fields employed were in the range 0–14 kG. Samples prepared in identical fashion as those used in the merry-go-round experiments were placed into the center of the gap of the electromagnet. A specifically desired magnetic field was produced by applying an electric current. Each sample was irradiated with a 450-W Oriel xenon lamp to appropriate conversions.

(23) Elderfield, R. C.; Meyer, V. B. *J. Am. Chem. Soc.* **1954**, *76*, 1883.
(24) Buehler, C. A.; Pearson, D. E. "Survey of Organic Synthesis"; Wiley-Interscience: New York, 1970; p 874.
(25) Roof, A .A. M.; vanWoerden, H. F.; Cerfontain, H. *J. Chem. Soc., Perkin Trans. 2* **1979**, 1545.
(26) Murov, S. L. "Handbook of Photochemistry"; Marcel Dekker: New York, 1973.

Analyses. 1. VPC Analysis. Micellar or aqueous ketone-saturated photolysis mixtures were extracted with calibrated volumes of ethyl ether (containing an internal standard, typically hexadecane or benzophenone) and then subjected to quantitative VPC analysis. Product analyses were performed with a 3% OV-17/chrom-Q column (6 ft × $^1/_8$ in., column temperature 160–200 °C for DBK and as high as 240 °C for higher molecular weight photoinitiators). Products from scavenging by Cu^{2+} were also analyzed, relative to a standard, by using a lower column temperature (105–160 °C (10 °C/min) for detection of benzyl chlorides and benzyl alcohols). All products were identified on the basis of the known photochemistry of starting material as well as the known retention times of authentic compounds.

Homogeneous photolysis mixtures composed of an organic solvent were typically treated with standard and then analyzed directly by VPC analysis (as described above).

2. VPC/MS Analysis. For VPC/MS analysis of micellar photolysis mixtures, products were extracted with ether and the organic layer was submitted for analysis. A Finnigan 3300 with data system 6000 equipped with an OV-101 column and temperature programmed (150–200 °C) was employed using electron impact as the method of analysis.

Data Treatment. Disappearance yields and product yields from photolyses were typically measured with respect to a standard. An unphotolyzed control sample was used to determine ketone disappearances as well as ensure proper mass balance of starting materials and products.

Quantum yield or cage effect (by scavenging, see eq 2 and 6) determinations routinely involved preparation of 2–3 sets of samples per measurement. Only the averages of these analyses were used in the calculations.

Acknowledgment. We thank the National Science Foundation and the Air Force Office of Scientific Research for their generous support of this research.

Registry No. DBK, 102-04-5; DBK-*2,2'*-$^2H_4$, 66223-95-8; DBK-*2,2'*-^{13}C, 77787-71-4; 4-Me-DBK, 35730-02-0; 4,4'-di-Me-DBK, 70769-70-9; 4,4'-di-*t*-Bu-DBK, 64321-35-3; DBK-*1*-^{13}C, 68120-92-3; 4-Cl-DBK, 35730-03-1; 4-Br-DBK, 65636-25-1; DBK-$^2H_{14}$, 84752-07-8; DBK-$^2H_{10}$, 84752-08-9; HDTCl, 112-02-7; DDTCl, 112-00-5; STS, 1191-50-0; SDS, 142-87-0; SDS, 142-31-4; SHS, 2207-98-9; $NaDodSO_4$, 151-21-3; $C_6D_5CD_2CO_2H$, 65538-27-4; $(PhCH_2)_2Cd$, 17051-04-6; $CdCl_2$, 10108-64-2; PNK, 31283-78-0; DNK, 51042-38-7; NaCl, 7647-14-5; $PhCH_2OH$, 100-51-6; Na_2SO_4, 7757-82-6; O_2, 7782-44-7; $CuCl_2$, 7447-39-4; ^{13}C, 14762-74-4; D, 7782-39-0; (4-methylphenyl)acetic acid, 622-47-9; benzyl chloride, 100-44-7; (4-methylphenyl)acetyl chloride, 35675-44-6; (4-chlorophenyl)acetyl chloride, 25026-34-0; (4-bromophenyl)acetyl chloride, 37859-24-8; (4-chlorophenyl)acetic acid, 1878-66-6; (4-bromophenyl)acetic acid, 1878-68-8; 4-*tert*-butylbenzyl bromide, 18880-00-7; 4-*tert*-butylbenzyl cyanide, 3288-99-1; (4-*tert*-butylphenyl)acetic acid, 32857-63-9; (4-*tert*-butylphenyl)acetyl chloride, 52629-45-5; 4-*tert*-butylbenzylcadmium, 84752-09-0; 1-naphthylacetyl chloride, 5121-00-6; 1-naphthylacetic acid, 86-87-3; 1-naphthylacetic anhydride, 5415-58-7.

Magnetic Circular Dichroism Determination of Zero-Field Splitting in Chloro(*meso*-tetraphenylporphinato)iron(III)

W. R. Browett,[1] A. F. Fucaloro,[1,2] T. V. Morgan,[1] and P. J. Stephens*[1]

Contribution from the Department of Chemistry, University of Southern California, University Park, Los Angeles, California 90089-0482. *Received July 19, 1982*

Abstract: The magnetic circular dichroism (MCD) spectrum of chloro(*meso*-tetraphenylporphinato)iron(III) [FeCl(TPP)] in dilute solution in polystyrene films has been measured over the temperature range 4–300 K. The MCD spectrum of this high-spin ($S = {}^5/_2$) complex is dominated by paramagnetic effects (*C* terms). The MCD temperature dependence at selected wavelengths is fit, assuming contributions from three ground-state Kramers doublets at energies 0, 2*D*, and 6*D*, where *D* is the quadratic axial zero-field splitting parameter. The *D* values obtained are independent of wavelength and in excellent agreement with previous measurements by other techniques. MCD is thus shown to be a usable technique for the determination of zero-field splitting parameters.

Introduction

Many complexes of transition-metal ions exhibit extremely low-lying excited electronic states at energies comparable to or less than thermal energies. Such electronic-state manifolds generally arise from the effects of small perturbations on otherwise degenerate states, and the splitting of this degeneracy is referred to as zero-field splitting. For example, in cubic complexes of first-row transition-metal ions, zero-field splittings are generally caused by noncubic (e.g., tetragonal, trigonal, rhombic) distortions and/or spin–orbit coupling.

The excited electronic states of a transition-metal complex are most commonly investigated by means of optical spectroscopy. However, the direct study of excited states of a zero-field split manifold requires the use of medium- or far-infrared (IR) spectroscopy, which is complicated by competition from vibrational absorption. Zero-field splittings are consequently more often studied by other techniques that make use of the thermal accessibility of the excited states. Such techniques include magnetic susceptibility and EPR, Mössbauer and NMR spectroscopies.

We discuss here the use of magnetic circular dichroism (MCD) in the determination of zero-field splittings. The MCD of a transition arises from the perturbation of ground and excited electronic states by a magnetic field.[3] In the case of a system with zero-field splitting, the net MCD is the summed effect of transitions from each level of the zero-field split manifold. The temperature (*T*) dependence of the MCD is then determined in part by the Boltzmann population factors of each level, which in turn reflect the zero-field splittings.

Despite extensive use of MCD for the study of ground and excited electronic states of transition-metal ions,[4] the use of MCD for the determination of zero-field splittings has been negligible for a variety of reasons. Instrumentation permitting extensive and facile sample-temperature variation has until relatively recently been available infrequently. Systems chosen for study at cryogenic temperatures have rarely exhibited zero-field splittings in the range accessible by MCD. In some cases where zero-field splittings exist, theoretical analysis of MCD data was not un-

(1) University of Southern California.
(2) Permanent address: Joint Science Department, Claremont Colleges, Claremont, CA 91711.

(3) P. J. Stephens, *Adv. Chem. Phys.*, **35**, 197 (1976).
(4) P. J. Stephens, *Ann. Rev. Phys. Chem.*, **25**, 201 (1974).

0002-7863/83/1505-1868$01.50/0